Effect of impurity scattering in nanoscale Corbino disks

Satofumi Souma and Akira Suzuki
Center for Solid-State Physics and Department of Physics, Faculty of Science, Science University of Tokyo, 1-3 Kagurazaka, Shinjuku-ku, Tokyo 162-8601, Japan
(Received 5 January 1998)

We have studied electrical conductance of nanoscale Corbino disks having single δ-function impurities. Kirczenow [J. Phys.: Condens. Matter **6**, L583 (1994)] predicted that the conductance G in ballistic Corbino disks at zero temperature is quantized in *odd* integer multiples of $2e^2/h$. We found that the same feature of conductance quantization as in the case of ballistic Corbino disks can be seen in the presence of single repulsive δ-function impurity in nanoscale Corbino disks, regardless of the impurity strength. For an attractive δ-function impurity, however, G decreases significantly at the energy levels of quasibound states formed in the effective confining potential. This indicates that the presence of evanescent modes strongly affects the scattering of propagating waves by single attractive δ-function impurity. This feature appears distinctively in the first step of the conductance for weak impurity whereas for strong impurity in the second or subsequent steps, depending on the strength of the impurity. [S0163-1829(98)03432-8]

I. INTRODUCTION

Recently, Kirczenow[1] proposed nanoscale Corbino disks whose characteristic dimensions are smaller than the mean free path of electrons. A Corbino disk is an annular region of conductor [an annular two-dimensional electron gas (2DEG) system] surrounding a metallic contact (i.e., an electrode) and surrounded in turn by a second metallic contact. This is schematically illustrated in Fig. 1(a). Unlike the macroscopic Corbino disks,[2,3] it is reasonable to expect that electrons in nanoscale Corbino disks at 0 K will be transported ballistically from one contact to the other without the influence of phonons and impurities. Kirczenow studied theoretically the transport properties of ballistic nanoscale Corbino disks with ideal contacts and showed that in the absence of magnetic fields, ballistic (impurity free) Corbino disks should exhibit conductance quantization in *odd* integer multiples of $2e^2/h$. This characteristic feature of conductance for an annular 2DEG system arises from those electrons that are in the eigenstates of angular momentum. Accordingly, those electrons are able to flow freely from inner to outer contact through the conduction channel of each mode l formed in a Corbino disk. Here, l denotes azimuthal modes and takes all integers. In the case of zero magnetic fields, two modes, $+|l|$ and $-|l|$, contribute to the transport in the same conduction channel. According to the Landauer formula, each channel contributes $2e^2/h$ to the conductance. Taking into account the contributions from modes $l=0$ and $|l|\geqslant 1$ to the conduction channels, one can thus easily understand the conductance quantization in Corbino disks. This conductance quantization in ballistic Corbino disks is analogous to that observed in ballistic quantum wires.[4–6] However, in quantum wires, *all* integer multiples of $2e^2/h$ are seen. This difference in conductance quantization arises from those electrons in quantum wires that flow the conduction channels opened for each mode n of the energy eigenstates in the direction of quantum well. Here, n takes any integer.

Many experimental and theoretical studies have been done on impurity scattering in quantum wires:[7–10] Bagwell[7,8] studied the effect of impurities on the conductance of quasi-one-dimensional wires and showed that the presence of evanescent modes strongly affects scattering of propagating modes from those impurities in such systems. The conductance quantization in ballistic Corbino disks is analogous to that in quantum wires. However, the essential difference between a Corbino disk and quantum wire lies in the geometry of their confinement potential since the boundaries of a Corbino disk consist entirely of metallic contacts so that there is no confinement potential. Thus, it is expected that the influence of impurity scattering in Corbino disks would be different from that in quantum wires. In this paper, the theoretical study of transport properties of nanoscale Corbino disks in the presence of impurities is presented. Our main

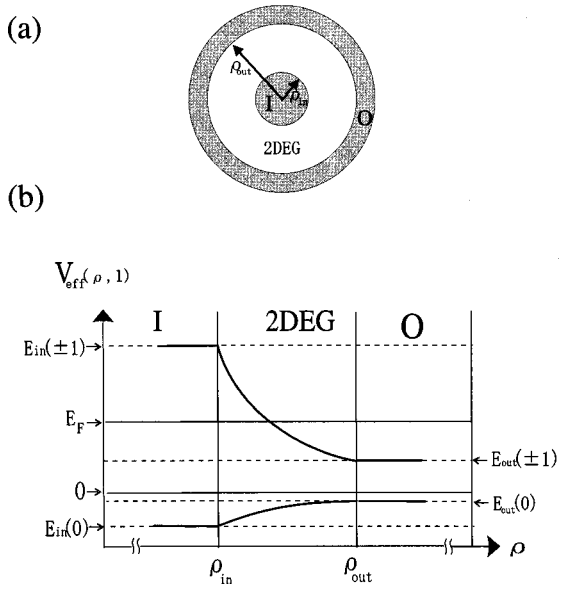

FIG. 1. (a) Schematic of a Corbino disk with inner and outer radii ρ_{in} and ρ_{out} of contacts. Shaded areas are electrodes (contacts). (b) Effective potential $V_{eff}(\rho,l)$ vs ρ for $l=0, \pm 1$. I and O represent inner contact and outer contact respectively.

goal in this paper is to understand the simplest possible scattering problem in nanoscale Corbino disks, that is, scattering from single δ-function impurity that destroys the symmetry of annular 2DEG. We will study how the conductance is influenced by the single δ-function impurity in a nanoscale Corbino disk with ideal contacts.

This paper is organized as follows. In Sec. II, a general theoretical treatment of the quantum transport is given for annular 2DEG systems with static impurities in the polar coordinates and an expression for the conductance is given for Corbino disks with single δ-function impurity on the basis of the Landauer-Büttiker formalism.[11,12] The results of numerical calculations for the conductance and their physical analysis are given in Sec. III. Actual numerical calculations are carried out by applying the method of transfer matrix, which is outlined in the Appendix. In the final section, we conclude with a brief summary of the results.

II. THEORY

Let us first consider the quantum-mechanical problem of 2D electron gas with static impurities in a (nanoscale) Corbino disk (i.e., an annular 2D conductor) without electrodes. Within the effective-mass approximation, the Schrödinger equation for an electron with effective mass m^* can be expressed in an appropriate form for the transport in the radial (ρ) direction as[13]

$$\left\{-\frac{\hbar^2}{2m^*}\frac{\partial^2}{\partial\rho^2}-\frac{\hbar^2}{2m^*\rho^2}\left(\frac{\partial^2}{\partial\theta^2}+\frac{1}{4}\right)+V_{\rm imp}(\rho,\theta)\right\}\eta(\rho,\theta) = E\,\eta(\rho,\theta), \tag{1}$$

where $V_{\rm imp}(\rho,\theta)$ denotes an impurity potential at (ρ,θ). It is clear that the first and the second terms on the left-hand side of Eq. (1) represent the radial (ρ) and the azimuthal (θ) component of the kinetic energy of an electron, respectively. The remaining term $(-\hbar^2/8m^*\rho^2)$ is the quantum-mechanical correction of potential, which arises due to the specific geometry of a Corbino disk.[13] To obtain expression (1), we made the simple transformation for the wave function $\psi(\rho,\theta)$ of the Schrödinger equation for an electron in the polar coordinates: $\psi(\rho,\theta)=\rho^{-1/2}\eta(\rho,\theta)$. Our problem seems to be reduced to a usual 1D potential-well problem if there were no impurity [i.e., $V_{\rm imp}(\rho,\theta)=0$]. In order to obtain the solutions $\eta(\rho,\theta)$ of Eq. (1) satisfying the boundary conditions of the Corbino disk, we shall apply the mode-matching method employed by Datta, Cahay, and McLennan[14] and Cahay, McLennan, and Datta[15] for their calculation of impurity scattering in the Cartesian coordinate system to the present problem in the circular polar coordinate system. When there is no impurity in the system, Eq. (1) can be easily separated in the variables to obtain the equation for $\Theta(\theta)$:

$$\frac{d^2}{d\theta^2}\,\Theta_l(\theta)=-l^2\Theta_l(\theta), \tag{2}$$

where l is an arbitrary constant. Imposing the periodic boundary condition for θ with a period 2π, l is given by $l=\ldots,-1,0,1,\ldots$. Since the normalized wave function $\Theta_l(\theta)=(1/\sqrt{2\pi})e^{il\theta}$ forms complete sets, an arbitrary function can be expanded in terms of $\Theta_l(\theta)$. Thus, we may express the solution of the Schrödinger Eq. (1) in the presence of impurity potential as

$$\eta(\rho,\theta)=\sum_{l=-\infty}^{+\infty}\Xi_l(\rho)\Theta_l(\theta). \tag{3}$$

Here, we note that the expansion coefficient $\Xi_l(\rho)$ is ρ dependent. By using Eq. (3) in Eq. (1), we obtain the equation for $\Xi_l(\rho)$:

$$\frac{d^2}{d\rho^2}\,\Xi_l(\rho)+\frac{2m^*}{\hbar^2}\{E-V_{\rm eff}(\rho,l)\}\Xi_l(\rho) = \sum_{m=-\infty}^{+\infty}\Gamma_{lm}(\rho)\Xi_m(\rho), \tag{4}$$

where $V_{\rm eff}(\rho,l)$ denotes an effective potential in the ρ direction and is given by

$$V_{\rm eff}(\rho,l)=\frac{\hbar^2}{2m^*\rho^2}\,(l^2-\tfrac{1}{4}). \tag{5}$$

Electrons in Corbino disks feel this potential actually. Since the $V_{\rm eff}(\rho,l)$ depends on l^2, it is degenerate with respect to the modes $\pm|l|$. $\Gamma_{lm}(\rho)$ indicates a coupling between modes l and m due to the presence of impurity (i.e., $V_{\rm imp}$) and is given by

$$\Gamma_{lm}(\rho)=\frac{2m^*}{\hbar^2}\int_0^{2\pi}d\theta\;\Theta_l^*(\theta)V_{\rm imp}(\rho,\theta)\Theta_m(\theta). \tag{6}$$

Eqs. (4)–(6) form the basic equations for further development of the theory of 2DEG with any impurity in the circular polar coordinates. In this paper, we shall consider the simple case of single δ-function impurity. For impurity potential $V_{\rm imp}$, we adopt

$$V_{\rm imp}(\rho,\theta)=(\gamma/\rho)\,\delta(\rho-\rho_{\rm imp})\,\delta(\theta-\theta_{\rm imp}). \tag{7}$$

Here, $(\rho_{\rm imp},\theta_{\rm imp})$ indicates a position of δ-function impurity in the 2D polar coordinates. γ denotes the strength of impurity potential, where $\gamma>0$ indicates a repulsive potential, whereas $\gamma<0$ an attractive potential. The coupling constant (6) for the δ-function impurity can be readily obtained by substituting Eq. (7) into Eq. (6) as

$$\Gamma_{lm}(\rho)=\tilde{\Gamma}_{lm}\delta(\rho-\rho_{\rm imp}), \tag{8}$$

where $\tilde{\Gamma}_{lm}$ is given by

$$\tilde{\Gamma}_{lm}=\frac{2m^*\gamma}{\hbar^2\rho_{\rm imp}}\,\Theta_l^*(\theta_{\rm imp})\Theta_m(\theta_{\rm imp}). \tag{9}$$

The above preliminary theory can be applied to the quantum transport of noninteracting electrons in a Corbino disk attached to metallic contacts (electrodes) [see Fig. 1(a)]. In order to study electronic transport properties in Corbino disks, it is, however, necessary to model the emission and absorption of electrons by the electrodes. In this paper, we adopt a model of ideal contacts employed by Kirczenow.[1] The model is constructed so that electrons may flow freely into and out of the contacts in mode l of the conduction

channel in a Corbino disk and any electrons that enter contacts are absorbed by the electrodes. This can be achieved by treating each electrode as if it were a two-dimensional system with l-dependent effective potential $V_{\rm eff}(\rho,l)$ defined in the region $\rho\in(0,\infty)$ by

$$V_{\rm eff}(\rho,l)=\begin{cases} E_{\rm in}(l)\equiv\dfrac{\hbar^2}{2m^*\rho_{\rm in}^2}\,(l^2-\frac{1}{4}) & \text{for } \rho\in(0,\rho_{\rm in}) \\ \dfrac{\hbar^2}{2m^*\rho^2}\,(l^2-\frac{1}{4}) & \text{for } \rho\in[\rho_{\rm in},\rho_{\rm out}] \\ E_{\rm out}(l)\equiv\dfrac{\hbar^2}{2m^*\rho_{\rm out}^2}\,(l^2-\frac{1}{4}) & \text{for } \rho\in(\rho_{\rm out},\infty), \end{cases} \tag{10}$$

where $\rho_{\rm in},\rho_{\rm out}$ denote the radii of inner and outer contacts, respectively. Thus, we must solve the Schrödinger Eq. (4) with the effective potential $V_{\rm eff}(\rho,l)$ under these conditions for the electronic transport in a Corbino disk. Since the solution of the Schrödinger equation inside the electrodes is accordingly given by the linear combination of two waves propagating to the $\pm\rho$ directions, an electron in the annular 2DEG entering the electrodes can never come back to the annular region attached to such ideal contacts.

Now, let us consider the solutions of the Schrödinger Eq. (4) with the effective potential (10). Schematic view of the effective potential $V_{\rm eff}(l,\rho)$ for $l=0,\pm1$ is given in Fig. 1(b). In order to obtain the solutions of Eq. (4), we solve it separately for mode l in the regions of $\rho\in(0,\rho_{\rm in})$, $\rho\in[\rho_{\rm in},\rho_{\rm imp})$, $\rho\in(\rho_{\rm imp},\rho_{\rm out}]$, and $\rho\in(\rho_{\rm out},\infty)$, and then impose the boundary conditions at $\rho=\rho_{\rm in}$, $\rho=\rho_{\rm imp}$, and $\rho=\rho_{\rm out}$ on those wave functions. It should be noted that in these regions, there is *no* effect due to the presence of the impurity [i.e., $\Gamma_{lm}=0$ in Eq. (4)]. The wave functions, $\Xi_l(\rho)$'s, in each region are given by

$$\Xi_l(\rho)=\begin{cases} \dfrac{a_l}{\sqrt{k_{l,\rm in}}}\,e^{ik_{l,\rm in}\rho}+\dfrac{b_l}{\sqrt{k_{l,\rm in}}}\,e^{-ik_{l,\rm in}\rho} & \text{for } \rho\in(0,\rho_{\rm in}) \\ e_l\rho^{1/2}Z_l(\alpha\rho)+f_l\rho^{1/2}\tilde{Z}_l(\alpha\rho) & \text{for } \rho\in[\rho_{\rm in},\rho_{\rm imp}) \\ g_l\rho^{1/2}Z_l(\alpha\rho)+h_l\rho^{1/2}\tilde{Z}_l(\alpha\rho) & \text{for } \rho\in(\rho_{\rm imp},\rho_{\rm out}] \\ \dfrac{c_l}{\sqrt{k_{l,\rm out}}}\,e^{ik_{l,\rm out}\rho}+\dfrac{d_l}{\sqrt{k_{l,\rm out}}}\,e^{-ik_{l,\rm out}\rho} & \text{for } \rho\in(\rho_{\rm out},\infty), \end{cases} \tag{11}$$

where $\alpha=\sqrt{2m^*|E|/\hbar^2}$ and $Z_l,\tilde{Z}_l$ are, respectively, defined by

$$Z_l(\alpha\rho)=J_l(\alpha\rho),\quad \tilde{Z}_l(\alpha\rho)=N_l(\alpha\rho)\quad \text{for } E\geqslant0, \tag{12}$$

$$Z_l(\alpha\rho)=I_l(\alpha\rho),\quad \tilde{Z}_l(\alpha\rho)=K_l(\alpha\rho)\quad \text{for } E<0.$$

Here, $J_l(x)$ denotes a Bessel function, $N_l(x)$ a Neumann function, $I_l(x)$ a modified Bessel function, and $K_l(x)$ a modified Neumann function.[16] The $k_{l,\rm in}$ and $k_{l,\rm out}$ in Eq. (11) are the radius wave vectors in the inner-contact and the outer-contact regions, respectively. For propagating modes $(E>E_{\rm in(out)})$, $k_{l,\rm in(out)}$ are given by

$$k_{l,\rm in(out)}=\left(\frac{2m^*\{E-E_{\rm in(out)}(l)\}}{\hbar^2}\right)^{1/2} =\left[k^2-\left(\frac{l}{\rho_{\rm in(out)}}\right)^2+\frac{1}{4\rho_{\rm in(out)}^2}\right]^{1/2}, \tag{13}$$

whereas for the evanescent modes $[E<E_{\rm in(out)}]$, $k_{l,\rm in(out)}$ are given by

$$k_{l,\rm in(out)}=i\left(\frac{2m^*\{E_{\rm in(out)}(l)-E\}}{\hbar^2}\right)^{1/2} =i\left[\left(\frac{l}{\rho_{\rm in(out)}}\right)^2-\frac{1}{4\rho_{\rm in(out)}^2}-k^2\right]^{1/2}\equiv i\kappa_{l,\rm in(out)}. \tag{14}$$

Here $k=\sqrt{2m^*E/\hbar^2}$ is the wave vector of an electron with energy E. For a given energy E, we write the largest mode l as $l^*_{\rm in(out)}$ such that the wave function becomes a propagating wave mode [i.e., $E>V_{\rm eff}(\rho_{\rm in(out)},l)$] at the inner (outer) contact.

$$l^*_{\rm in(out)}=\mathrm{Int}\left[\left(\frac{2m^*E}{\hbar^2}\,\rho_{\rm in(out)}^2+\frac{1}{4}\right)^{1/2}\right]. \tag{15}$$

Here Int$[x]$ represents the largest integer that is smaller than x. It should be noted that $l^*_{\rm out}$ is always greater than $l^*_{\rm in}$. These wave functions $\Xi_l(\rho)$ given in Eq. (11) must satisfy the following boundary conditions for the continuity of the wave functions:

$$\Xi_l(\rho-0)=\Xi_l(\rho+0),\qquad \left.\frac{d\Xi_l(\rho)}{d\rho}\right|_{\rho-0}=\left.\frac{d\Xi_l(\rho)}{d\rho}\right|_{\rho+0}\quad \text{at } \rho_{\rm in},\rho_{\rm out} \tag{16}$$

and

$$\Xi_l(\rho_{\rm imp}-0)=\Xi_l(\rho_{\rm imp}+0),$$
$$\left.\frac{d\Xi_l(\rho)}{d\rho}\right|_{\rho_{\rm imp}+0}-\left.\frac{d\Xi_l(\rho)}{d\rho}\right|_{\rho_{\rm imp}-0}=\sum_{m=-\infty}^{\infty}\tilde{\Gamma}_{lm}\Xi_m(\rho_{\rm imp}). \tag{17}$$

It is noted that each mode l is *not* independent but coupled with another mode m $(\neq l)$ (i.e., $\tilde{\Gamma}_{lm}\neq 0$ for $l\neq m$) at $\rho=\rho_{\rm imp}$. This is because the circular symmetry is destroyed by the impurity in the system. Imposing these continuity conditions [Eqs. (16) and (17)] on the wave function $\Xi_l(\rho)$ in Eq. (11) at the boundaries ($\rho=\rho_{\rm in(out)}$ and $\rho=\rho_{\rm imp}$) and also the normalization condition for $\Xi_l(\rho)$, we can in principle determine a set of parameters $(a_l,b_l,c_l,d_l,e_l,f_l,g_l,h_l)$ for a given electron energy E. The summation on the right-hand side of Eq. (17) includes the infinite number of coupled modes, so that one must solve the infinite dimensional simultaneous equations to obtain the exact value of those parameters $(a_l,\ldots,h_l)$.

The transmission coefficient T_{nl} from a propagating mode n $(<l^*_{\rm in})$ in the inner contact to a propagating mode l $(<l^*_{\rm out})$ in the outer contact can be expressed as

$$T_{nl}=\left|\frac{c_l}{a_n}\right|^2. \tag{18}$$

It should be noted again that one must take into account the infinite number of coupled modes to obtain the exact answer for T_{nl}. The conductance can be related to a transmission coefficient through the Landauer-Büttiker formula for multichannels.[11,12] The conductance G of Corbino disks is thus given by

$$G=\frac{2e^2}{h}\sum_{n=-l^*_{\rm in}}^{l^*_{\rm in}}\sum_{l=-l^*_{\rm out}}^{l^*_{\rm out}}T_{nl}, \tag{19}$$

where T_{nl} is given by Eq. (18). Actual numerical calculation of the T_{nl} can be carried out by the method of transfer matrix[17,18] in which we have taken the summation in Eq. (17) up to $|m|=N_c$. (See the Appendix.) Here N_c should be large enough to include sufficient evanescent modes. We note here that the transmission coefficient T_{nl} is then given as a function of Fermi energy.

III. RESULTS AND DISCUSSION

The zero-temperature conductance G of a nanoscale Corbino disk in the presence of single δ-function impurity is calculated as a function of the Fermi energy E_F for various cases by making use of Eq. (19) along with Eq. (18) (see also the Appendix).

A. Repulsive impurity

Figure 2 shows Fermi-energy dependence on the conductance in the case of repulsive impurity with different strengths γ at $\rho_{\rm imp}=(\rho_{\rm in}+\rho_{\rm out})/2$ for the case $\rho_{\rm out}/\rho_{\rm in}=1.1$. The Fermi energy is scaled by $E_{\rm in}(1)$ in the lower axis and by $E_{\rm out}(1)$ in the upper axis, where $E_{\rm in(out)}(1)$ is defined by Eq. (10). Thus, the effective potential of mode l at the inner (outer) contact (which we refer to the lth subband energy) is expressed by $(4l^2-1)/3$ in the lower (upper) axis of the

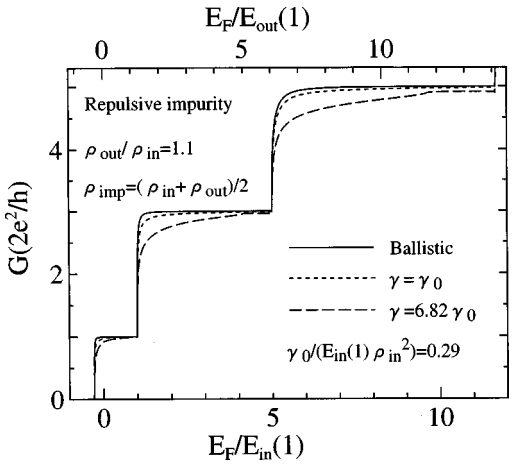

FIG. 2. Conductance G vs Fermi energy E_F for nanoscale Corbino disk with single repulsive δ-function impurity. Impurity is located at $\rho_{\rm imp}=(\rho_{\rm in}+\rho_{\rm out})/2$. Conductance G is scaled by $2e^2/h$.

figure. We have used the effective mass of an electron as $m^*=0.067m_0$ for GaAs in this paper. In the presence of single δ-function impurity, the θ component of the impurity position ($\theta_{\rm imp}$) does *not* affect the conductance due to the geometric symmetry of the Corbino disk. The strengths of the impurity are listed in the figure. For comparison, the conductance for the ballistic (impurity-free) case is drawn as a solid line. The conductance is zero in the energy region $E_F<E_{\rm out}(0)$ for which the lowest mode $l=0$ cannot flow from inner contact to outer contact. The ballistic conductance increases step wisely at each $E_{\rm in}(1,2,\ldots)$ and is approximately given by $G=(2e^2/h)(2l^*_{\rm in}+1)$ as discussed by Kirczenow.[1] Here $l^*_{\rm in}$ is given by Eq. (15). Due to the reflection by the spatially varying effective potential $V_{\rm eff}$, the conductance curve is rounded even in the ballistic case. As seen in the figure, the repulsive impurity does *not* alter the qualitative behavior of the ballistic conductance though it decreases slightly due to the increase of the reflection by the impurity potential. Interestingly, the conductance is less affected by the repulsive impurity in the energy region of $E_{\rm out}(l)<E_F<E_{\rm in}(l)$ for each l. In this energy region, there are in general more than one propagating mode in the outer contact than in the inner contact. Therefore, an electron with energy $E\in[E_{\rm out}(l),E_{\rm in}(l)]$ incoming from inner contact can be transmitted into outer contact easily.

B. Attractive impurity

Figures 3(a) and 3(b) show Fermi-energy dependence on the conductance in the case of attractive impurity. The same values of $\rho_{\rm imp}$ and $\rho_{\rm out}/\rho_{\rm in}$ are used as in Fig. 2. Being different from the case for repulsive impurity, the conductance quantization is significantly affected by the presence of single-attractive impurity, and also by its strength. Let us first consider the case for weak (shallow) impurity having $\gamma=-\gamma_0$ $[=-0.29E_{\rm in}(1)\rho^2_{\rm in}]$ [dotted line in Fig. 3(a)]. In this case, we can see that the conductance is zero just below the energy at $E_{\rm out}(1)$. In this energy, as seen in Fig. 1(b), there is only one propagating mode $l=0$. Hence, the intramode transmission probability of mode $l=0$ is zero at that energy. This anomalous decrease in the transmission prob-

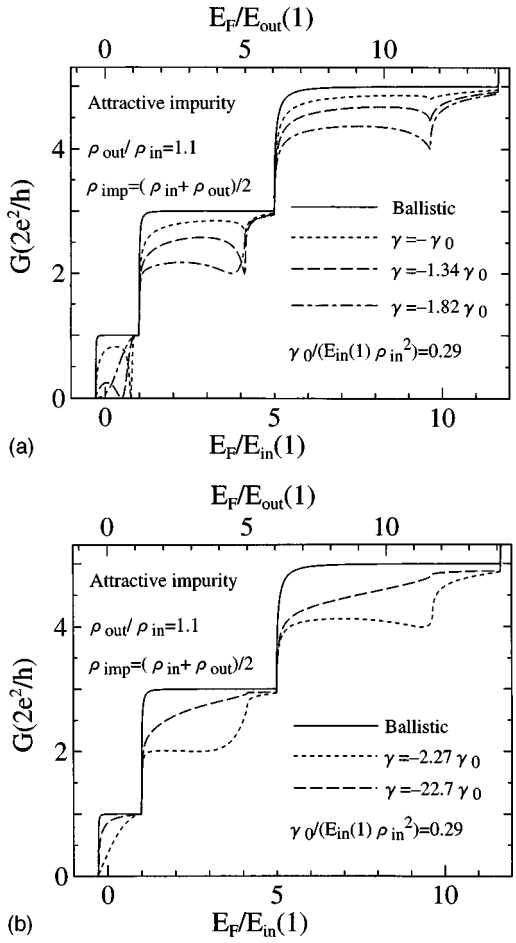

FIG. 3. Conductance G vs Fermi energy E_F for nanoscale Corbino disk with single attractive δ-function impurity for five different strengths. Conductance G is scaled by $2e^2/h$.

ability can be realized by taking into account the evanescent modes. As seen in Eq. (4), the potential energy felt by an electron is actually given by the sum of effective potential $V_{\text{eff}}(\rho,l)$ and impurity potential V_{imp}. The lowest value of the effective potential $V_{\text{eff}}(\rho,l=\pm 1)$ is $E_{\text{out}}(1)$ as seen in Fig. 1(b). Thus, weak attractive impurity potential formed in the effective potential $V_{\text{eff}}(\rho,l)$ has a bound energy just below $E_{\text{out}}(1)$. Therefore, an electron with energy just below $E_{\text{out}}(1)$ cannot flow through the propagating mode $l=0$ since the electron is bounded by the potential well formed in the effective potential $V_{\text{eff}}(\rho,1)$. That is why the transmission probability in this case is zero. This bound state is called *quasibound* state and is essentially the same as one observed in quantum wires.[7,8] However, in the case of Corbino disks, the appearance of dips in the conductance is very different in each step. In the case of the weakest attractive impurity [dotted line in Fig. 3(a)], we can see the dip in the second and the third step as well just below $E_{\text{out}}(2)$ and $E_{\text{out}}(3)$, respectively. These dips are, however, not so deep as the first one. This feature can be explained as follows. Since the spatial variation of V_{eff} becomes larger for larger l, it is hard for weak attractive impurity potential to confined an electron in the effective potential V_{eff} for large l. That is why the dip in the second and third step is shallow. When we increase the strength of attractive impurity, the dip in the first step of the conductance shifts to the lower-energy side and the dip in the

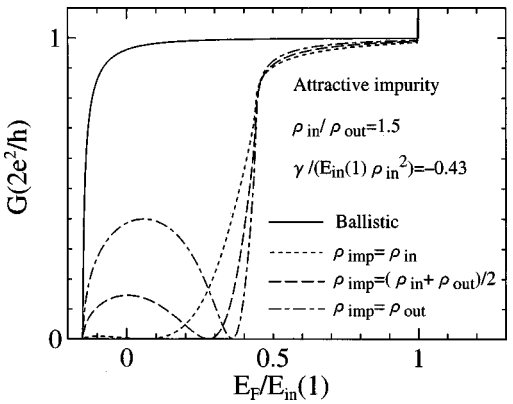

FIG. 4. Conductance G vs Fermi energy E_F for nanoscale Corbino disk with single attractive δ-function impurity at three different positions of the impurity. Conductance G is scaled by $2e^2/h$.

second step becomes deeper, at which the conductance is $2\times 2e^2/h$. In this case, the quasibound state is formed just below $E_{\text{out}}(2)$ even though the spatial variation of $V_{\text{eff}}(\rho,2)$ is large since the strength of the impurity is made stronger. It should be noted that since we assumed attractive ''δ-function'' impurity, the maximum decrease of the conductance due to the quasibound state is $2e^2/h$. The dip in the third step is thus still shallow.

Next we consider the case for an impurity with strength $\gamma=-1.82\gamma_0$ [dash-dotted line in Fig. 3(a)]. In this case, the quasibound state drops below the bottom energy of the first step and the dip in the first step disappears. The dip in the second step shifts to the lower-energy side and the dip in the third step becomes deeper, at which the conductance is $4\times 2e^2/h$. When we further increase the strength of the impurity [dotted line in Fig. 3(b)], the conductance in the first step increases because the quasibound state does not influence the first step of the conductance in this case. Then the dip in the second step disappears. As a whole, as the strength of the attractive impurity is increased, the effect of the quasibound state appears especially in the higher step, while the effect in the lower step becomes weak. The dashed line in Fig. 3(b) shows the case for the very strong attractive impurity. In this case the impurity potential is so strong that the first three steps of the conductance are not influenced by the quasibound state and the conductance curve resembles one in the case of the strong repulsive impurity (cf. Fig. 2).

C. Impurity position dependence on the conductance

Next, we consider the Corbino disk with $\rho_{\text{out}}/\rho_{\text{in}}=1.5$. In this case the effective potential $V_{\text{eff}}(\rho,l)$ varies from ρ_{in} to ρ_{out} greatly as compared with the case for $\rho_{\text{out}}/\rho_{\text{in}}=1.1$. Thus, in the case of weak attractive impurity, the effect of the quasibound state appears in the first step of the conductance distinctively. In Fig. 4 we show the position dependence on the conductance for weak attractive δ-function impurity. Since we are interested in the effect of the quasibound state, we show only the first step of the conductance in this figure. As seen in the figure, as the position of impurity ρ_{imp} approaches inner contact, the dip due to the quasibound state shifts to the lower-energy side. This feature can be explained as follows. In the circular polar coordinates the δ-function impurity is expressed by Eq. (7), which contains $1/\rho$. Thus,

in the 1D-like Schrödinger Eq. (4), the impurity potential behaves like $1/\rho_{\rm imp}$. Therefore, the effect of the impurity becomes strong when the impurity is put near the inner contact, while it becomes weak when the impurity is put near the outer contact. That is why the dip shifts lower in energy as the position of attractive δ-function impurity approaches inner contact. Due to the same reason, the conductance decreases slightly when single repulsive δ-function impurity is put near the inner contact, but its overall feature does not alter.

IV. CONCLUSION

In this paper, we have shown quantum-mechanical treatment of 2D electronic system with any impurity potential in the polar coordinates, and studied the electronic transport problems of a Corbino disk (i.e., annular 2DEG) with single δ-function impurity. On the basis of Landauer-Büttiker formalism,[11,12] we derived the formula for conductance of a Corbino disk by assuming ideal contacts (electrodes) proposed by Kirczenow.[1] Actual numerical calculations of the conductance were carried out by utilizing a method of transfer matrix.[17,18]

In the case where single repulsive δ-function impurity is present in nanoscale Corbino disk, we found that the conductance changes stepwise at the energies where new conduction channels are opened as in the ballistic case. Even in the case where the strength of the impurity is strong, the qualitative feature of the conductance remains the same. This indicates that the presence of single repulsive δ-function impurity does not alter the conductance quantization and the qualitative feature for the ballistic case significantly. On the other hand, in the presence of single-attractive δ-function impurity, the qualitative behavior of the conductance is different from the ballistic case due to the quasibound states formed by the presence of attractive impurity. This is because electrons are actually bounded by the potential well formed by the effective potential $V_{\rm eff}$ and the impurity potential $V_{\rm imp}$. Above all, the dips in the conductance appear at the energies of quasibound states in the potential well. In a Corbino disk, the effective potential varies with ρ^{-2} and its variation from $\rho_{\rm in}$ to $\rho_{\rm out}$ is larger for large l. Accordingly, the quasibound states due to the attractive impurity are hard to be formed in the effective potential with large l. As a result, the dip of the conductance appears distinctively in the first step of the conductance for weak (shallow) impurity whereas for strong (deep) impurity it appears in the second or subsequent steps, depending on the strength of the impurity. Finally, the effect of the quasibound state due to the presence of attractive impurity is strong when the impurity is put near the inner contact, resulting in the dip shifting to the lower-energy side.

In this paper, we have presented the first theoretical study of the transport properties of nanoscale Corbino disks with single δ-function impurity. It is hoped that this work will stimulate interest in these systems and facilitate future experiments.

APPENDIX

The method of transfer matrix is outlined to calculate the conductance numerically in the present system. In Eq. (11), we express the coefficients of the wave function $\Xi_l(\rho)$ in the electrodes in terms of the $(2N_c+1)$-component vectors:

$$\begin{aligned}
\mathbf{a}^\dagger &= \{a_{-N_c}, a_{-N_c+1}, \ldots, a_0, \ldots, a_{N_c-1}, a_{N_c}\},\\
\mathbf{b}^\dagger &= \{b_{-N_c}, b_{-N_c+1}, \ldots, b_0, \ldots, b_{N_c-1}, b_{N_c}\},\\
\mathbf{c}^\dagger &= \{c_{-N_c}, c_{-N_c+1}, \ldots, c_0, \ldots, c_{N_c-1}, c_{N_c}\},\\
\mathbf{d}^\dagger &= \{d_{-N_c}, d_{-N_c+1}, \ldots, d_0, \ldots, d_{N_c-1}, d_{N_c}\}.
\end{aligned} \tag{A1}$$

Here, N_c is a cutoff mode satisfying $N_c \gg l^*_{\rm in}$, $l^*_{\rm out}$ for $l^*_{\rm in,(out)}$ defined by Eq. (15). Then, the $2(2N_c+1)$-component vectors $(\mathbf{a},\mathbf{b})^\dagger$ and $(\mathbf{c},\mathbf{d})^\dagger$ are related to the $2(2N_c+1)\times 2(2N_c+1)$ transfer matrix $\hat{M}$:

$$\begin{pmatrix} \mathbf{a} \\ \mathbf{b} \end{pmatrix} = \hat{M} \begin{pmatrix} \mathbf{c} \\ \mathbf{d} \end{pmatrix}, \tag{A2}$$

where $\hat{M}$ is defined by

$$\begin{aligned}
\hat{M} = {} & \hat{P}^{-1}(\rho_{\rm in})\hat{Q}(\alpha\rho_{\rm in})\hat{Q}^{-1}(\alpha\rho_{\rm imp})\\
& \times\{\hat{Q}(\alpha\rho_{\rm imp}) - \hat{\Gamma}(\alpha\rho_{\rm imp})\}\hat{Q}^{-1}(\alpha\rho_{\rm out})\hat{P}(\rho_{\rm out}).
\end{aligned} \tag{A3}$$

Each matrix, $\hat{P}(x)$, $\hat{Q}(x)$, and $\hat{\Gamma}(x)$, expresses a $2(2N_c+1)\times 2(2N_c+1)$ matrix. $\hat{P}(x)$ is defined as

$$\hat{P}(x) = \begin{pmatrix} \hat{P}_{++}(x) & \hat{P}_{+-}(x) \\ \hat{P}_{-+}(x) & \hat{P}_{--}(x) \end{pmatrix}. \tag{A4}$$

It is noted that the elements of $\hat{P}(x)$, $\hat{P}_{++}(x)$, $\hat{P}_{+-}(x)$, $\hat{P}_{-+}(x)$, and $\hat{P}_{--}(x)$, represent the $(2N_c+1)\times(2N_c+1)$ matrix, and they are given by

$$\begin{aligned}
\{\hat{P}_{++}(x)\}_{lm} &= \{\hat{P}_{+-}(x)\}_{lm} = \frac{1}{\sqrt{k_l(x)}}\,\delta_{lm},\\
\{\hat{P}_{-+}(x)\}_{lm} &= i\sqrt{k_l(x)}\,\delta_{lm},\\
\{\hat{P}_{--}(x)\}_{lm} &= -i\sqrt{k_l(x)}\,\delta_{lm},
\end{aligned} \tag{A5}$$

respectively. Here, $k_l(x)$ is the wave vector of an electron and is given by $k_l(x) = \sqrt{2m^*[E - V_{\rm eff}(x,l)]/\hbar^2}$. Similarly, the matrix $\hat{Q}(x)$ is defined as

$$\hat{Q}(x) = \begin{pmatrix} \hat{Q}_{++}(x) & \hat{Q}_{+-}(x) \\ \hat{Q}_{-+}(x) & \hat{Q}_{--}(x) \end{pmatrix}, \tag{A6}$$

where

$$\begin{aligned}
&\{\hat{Q}_{++}(x)\}_{lm} = \zeta_l(x)\,\delta_{lm}, \quad \{\hat{Q}_{+-}(x)\}_{lm} = \tilde{\zeta}_l(x)\,\delta_{lm},\\
&\{\hat{Q}_{-+}(x)\}_{lm} = \zeta'_l(x)\,\delta_{lm}, \quad \{\hat{Q}_{--}(x)\}_{lm} = \tilde{\zeta}'_l(x)\,\delta_{lm}.
\end{aligned} \tag{A7}$$

It is noted that $\zeta_l(x)$ and $\tilde{\zeta}_l(x)$ are actually given by

$$\zeta_l(x) = \sqrt{x}Z_l(x), \quad \tilde{\zeta}_l(x) = \sqrt{x}\tilde{Z}_l(x), \tag{A8}$$

and $\zeta_l'(x)$ and $\tilde{\zeta}_l'(x)$ express the first derivative of $\zeta_l(x)$ and $\tilde{\zeta}_l(x)$ with respect to x, respectively. Here, $Z_l(x)$, $\tilde{Z}_l(x)$ are defined by Eq. (12). The $\hat{\Gamma}(x)$ in Eq. (A3) can be also expressed by

$$\hat{\Gamma}(x)=\begin{pmatrix}\hat{\Gamma}_{++}(x) & \hat{\Gamma}_{+-}(x)\\ \hat{\Gamma}_{-+}(x) & \hat{\Gamma}_{--}(x)\end{pmatrix}, \tag{A9}$$

where

$$\begin{aligned}\{\hat{\Gamma}_{++}(x)\}_{lm}&=\{\hat{\Gamma}_{+-}(x)\}_{lm}=0,\\ \{\hat{\Gamma}_{-+}(x)\}_{lm}&=\tilde{\Gamma}_{lm}\zeta_m(x),\\ \{\hat{\Gamma}_{--}(x)\}_{lm}&=\tilde{\Gamma}_{lm}\tilde{\zeta}_m(x).\end{aligned} \tag{A10}$$

Accordingly, the transfer matrix $\hat{M}$ can be also expressed in terms of four submatrices $(M_{++},M_{+-},M_{-+},M_{--})$ as

$$\hat{M}=\begin{pmatrix}\hat{M}_{++} & \hat{M}_{+-}\\ \hat{M}_{-+} & \hat{M}_{--}\end{pmatrix}. \tag{A11}$$

Here, each submatrix has $(2N_c+1)\times(2N_c+1)$ elements. The transmission coefficient from a propagating mode n $(<l_{\rm in}^*)$ in the inner contact $(\rho_{\rm in})$ to a propagating mode l $(<l_{\rm out}^*)$ in the outer contact $(\rho_{\rm out})$ can thus be expressed by

$$T_{nl}=\left|\frac{c_l}{a_n}\right|^2=|\{\hat{M}_{++}^{-1}\}_{l,n}|^2. \tag{A12}$$

By making use of Eq. (A12) and the Landauer-Büttiker formula[11,12] for multichannels, conductance G of Corbino disks can be evaluated from

$$G=\frac{2e^2}{h}\sum_{n=-l_{\rm in}^*}^{l_{\rm in}^*}\sum_{l=-l_{\rm out}^*}^{l_{\rm out}^*}T_{nl}=\frac{2e^2}{h}\sum_{n=-l_{\rm in}^*}^{l_{\rm in}^*}\sum_{l=-l_{\rm out}^*}^{l_{\rm out}^*}|\{\hat{M}_{++}^{-1}\}_{l,n}|^2, \tag{A13}$$

where the transmission coefficient T_{nl} should be calculated at the Fermi energy E_F. In the numerical calculation, we have chosen $N_c=7$ throughout this paper.

[1] G. Kirczenow, J. Phys.: Condens. Matter **6**, L583 (1994).
[2] R. B. Laughlin, Phys. Rev. B **23**, 5632 (1981).
[3] B. I. Halperin, Phys. Rev. B **25**, 2185 (1982).
[4] B. J. van Wees, H. Van Houten, C. W. J. Beenakker, J. G. Williamson, L. P. Kouwenhoven, D. van der Marel, and C. T. Foxon, Phys. Rev. Lett. **60**, 848 (1988).
[5] D. A. Wharam, T. J. Thornton, R. Newbury, M. Pepper, H. Ahmed, J. E. F. Frost, D. G. Hasko, D. C. Peacock, D. A. Ritchie, and G. A. C. Jones, J. Phys. C **21**, L209 (1989).
[6] G. Kirczenow, J. Phys.: Condens. Matter **1**, 305 (1989).
[7] P. F. Bagwell, Phys. Rev. B **41**, 10 354 (1990).
[8] P. F. Bagwell, J. Phys.: Condens. Matter **2**, 6179 (1990).
[9] C. S. Chu and R. S. Sorbello, Phys. Rev. B **40**, 5941 (1989).
[10] J. Masek, P. Lipavsky, and B. Kramer, J. Phys.: Condens. Matter **1**, 6395 (1989).
[11] R. Landauer, Philos. Mag. **21**, 863 (1970).
[12] M. Büttiker, Y. Imry, R. Landauer, and S. Pinhas, Phys. Rev. B **31**, 6207 (1985).
[13] A. Suzuki and S. Matsutani, Nuovo Cimento B **111**, 593 (1996).
[14] S. Datta, M. Cahay, and M. McLennan, Phys. Rev. B **36**, 5655 (1987).
[15] M. Cahay, M. McLennan, and S. Datta, Phys. Rev. B **37**, 10 125 (1988).
[16] G. Arfken, *Mathematical Methods for Physicists*, 2nd ed. (Academic, New York, 1970).
[17] A. V. Tartakovski, Phys. Rev. B **52**, 2704 (1995).
[18] B. Y. Gu and C. Basu, Int. J. Mod. Phys. B **9**, 3085 (1995).